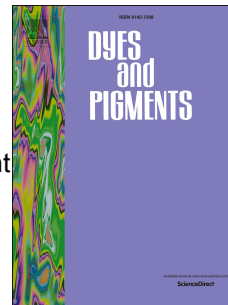


Accepted Manuscript

Fluorescent photochromic donor-acceptor Stenhouse adduct controlled by visible light

Shun Yang, Jing Liu, Zhanqi Cao, Mingming Li, Qianfu Luo, Dahui Qu



PII: S0143-7208(17)31831-4

DOI: [10.1016/j.dyepig.2017.09.040](https://doi.org/10.1016/j.dyepig.2017.09.040)

Reference: DYPI 6265

To appear in: *Dyes and Pigments*

Received Date: 29 August 2017

Revised Date: 15 September 2017

Accepted Date: 15 September 2017

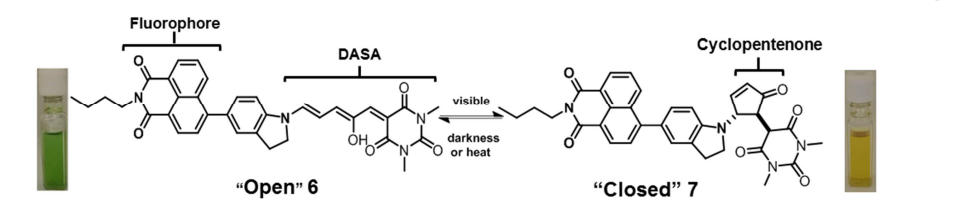
Please cite this article as: Yang S, Liu J, Cao Z, Li M, Luo Q, Qu D, Fluorescent photochromic donor-acceptor Stenhouse adduct controlled by visible light, *Dyes and Pigments* (2017), doi: 10.1016/j.dyepig.2017.09.040.

This is a PDF file of an unedited manuscript that has been accepted for publication. As a service to our customers we are providing this early version of the manuscript. The manuscript will undergo copyediting, typesetting, and review of the resulting proof before it is published in its final form. Please note that during the production process errors may be discovered which could affect the content, and all legal disclaimers that apply to the journal pertain.

Graphical Abstract

Fluorescent Photochromic Donor-Acceptor Stenhouse Adducts Controlled by Visible Light

by Shun Yang, Jing Liu, Zhanqi Cao, MingMing Li, Qianfu Luo*, Dahui Qu*



Fluorescent Photochromic Donor-Acceptor Stenhouse Adduct Controlled by Visible Light

Shun Yang^a, Jing Liu^a, Zhanqi Cao^{ab}, Mingming Li^a, Qianfu Luo^{*a}, Dahui Qu^{*a},

^a Key Laboratory for Advanced Materials and Institute of Fine Chemicals, East China University of Science and Technology, 130 Meilong Road, Shanghai, 200237, China.

^b College of Sciences, Henan Agricultural University, Zhengzhou 450002, China

Abstract: A novel photochromic fluorescent DASA (donor-acceptor Stenhouse adduct) switch controlled by visible light was successfully designed and synthesized. Using 1,8-naphthalimide fluorophore in combination with indoline-based “donor” and barbituric acid “acceptor”, the DASA molecule exhibits two independent absorption bands at 440 nm and 616 nm. The physical and thermodynamic properties of fluorescent donor-acceptor Stenhouse adduct (DASA-NDI) have been investigated in different solvents. In accordance with the unique fluorescent properties under visible light/heat and H^+/Cu^{2+} , using fluorescence intensity at 604 nm (I_{604}) as an output and visible light, H^+ and Cu^{2+} as inputs, a combinatorial logic gate consisting of NOR and AND logics can be described and operated.

Key words: Fluorescence; Photochromism; DASA; Logic gate

Introduction

Fluorescence, which is one of the most convenient and sensitive tools for investigating molecular features, has various practical applications, such as microanalysis [1] and bioimaging [2]. Typically, to avoid interference from other fluorophores in complex system, light-controlled molecular switches can be introduced, through which their applications including monitoring dynamic processes in real time, can be extend [3] and optical information can be stored in memory media [4]. Over the past few decades, chemists have synthesized various photochromic groups, such as spiropyran [5], diarylethene [6], azobenzene [7] and others [8-10]. However, most photochromic molecules either exhibit no fluorescence or show very

weak fluorescence, so introducing a fluorescent unit into the photochromic molecule is a common approach to change the fluorescent property. Upon irradiation with UV or visible light, the enhancement or extinction of fluorescence is achieved by energy-transfer or electro-transfer processes between fluorophores and photochromic groups, which have been proved to be versatile as fluorescent information storage [11], logic gates [12], cell imaging [13], and electro-optic devices [14].

The second generation aniline-based donor-acceptor Stenhouse adducts (DASAs) have recently been reported by Read de Alaniz and co-workers as a new class of visible light controlled molecular switches [15]. In contrast to the previously mentioned photoswitches which generally require UV irradiation to induce their photoisomerization, the photochromic progress of DASAs is caused by visible light, which is favorable for the application in biological systems [16-19]. Besides, this new photochromic switch provides a wide photoreponsive region from 500 nm to 650 nm that is not limited to solution-state or nonpolar matrices for reversible switching properties [20]. Moreover, the closed form of DASAs contains a cyclopentenone group which results in the occurrence of steric hindrance, affecting the formation of coordination compounds between copper ions (II) and the central nitrogen atoms [21, 22]. Significantly, upon addition of acid, the photochromic property of DASAs are different compared with the two former isomers [23]. Consequently, the significant changes in molecular structure and physicochemical properties associated with this isomerization process make DASAs become attractive candidates for the use as orthogonal photoswitch [24], actuators for drug delivery [19, 25], colorimetric

detection [23, 26] and spatiotemporal photopatterning [27, 28]. However, to the best of our knowledge, the combination of DASAs and fluorophores triggered by visible light has not been previously reported.

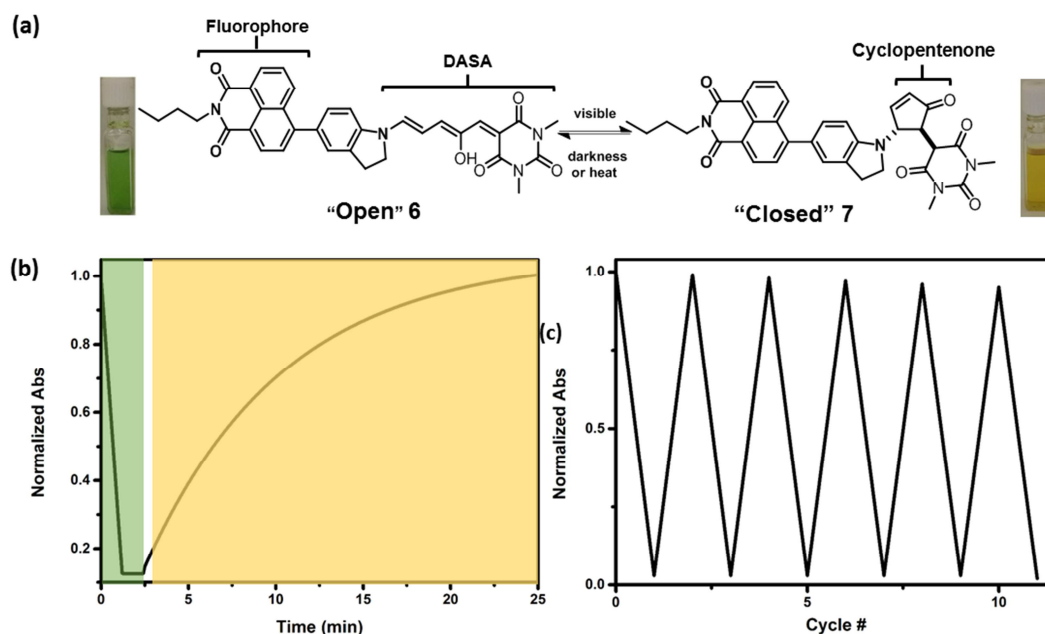


Figure 1. (a) The schematic representation of the two isomers **6**, **7** of the **DASA-NDI** under visible light and darkness or heat. (b) In situ kinetic plot of the switching cycle of **DASA-NDI** in CHCl_3 , monitored at $\lambda_{\text{max}} = 604$ nm and 35°C ; (c) Multiple photoswitching cycles of **DASA-NDI** showing 5% decrease in absorption after 10 cycles.

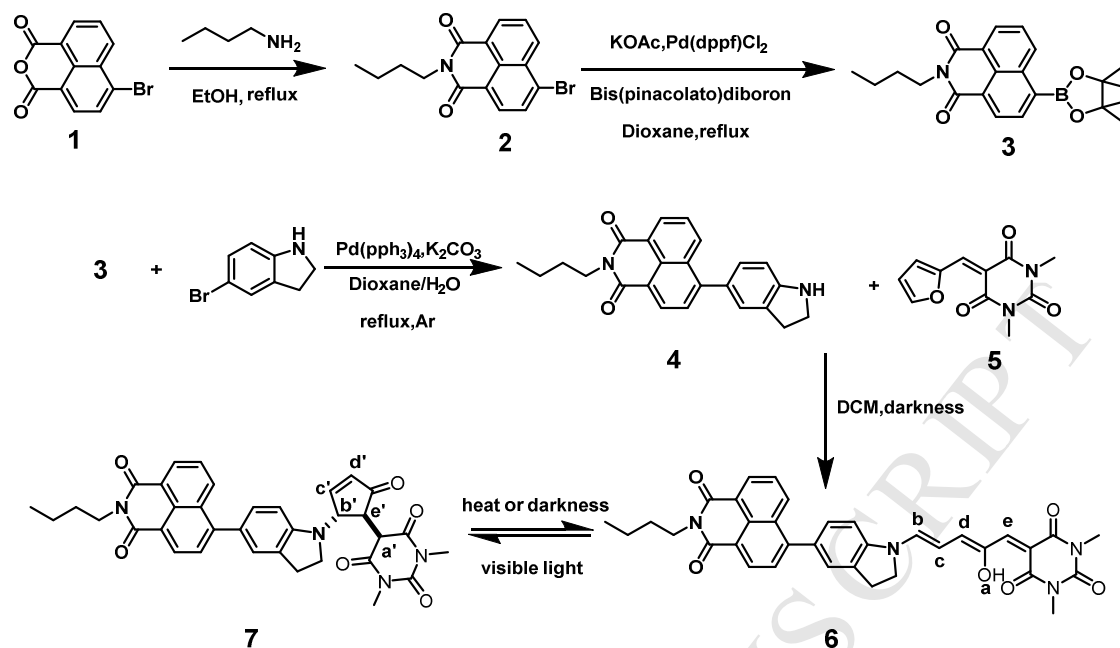
Herein we reported a second generation DASA and a 1,8-naphthalimide fluorophore are combined by Suzuki-Miyaura coupling, as shown in Figure 1. Upon irradiation with visible light, the thermodynamically unstable green “open” isomer **6** can be converted into the photostationary yellow “closed” isomer **7** with the fluorescence intensity of **DASA-NDI** increasing significantly. Moreover, the photochromic and fluorescent properties of **DASA-NDI** in different solvents were investigated and unique fluorescent properties under irradiation with certain wavelengths of visible light/heat and addition of $\text{H}^+/\text{Cu}^{2+}$ were discussed. Finally, based on its significant advantages, **DASA-NDI** can be applied as a reversible fluorescent photoswitch and a

combinatorial (NOR and AND) logic gate, where the Cu^{2+} , H^+ and visible light act as input, and the fluorescence intensity acts as output.

2 Experimental section

2.1 Materials and instrumentation

All chemicals were used as received from Adamas-beta, Acros, Aldrich, or Merck. All solvents were reagent grade, which were dried and distilled prior to use according to standard procedures. The molecular structures of the unknown compounds were confirmed via ^1H NMR, ^{13}C NMR and High Resolution ESI mass spectroscopy. ^1H NMR spectra and ^{13}C NMR were recorded on a Brücker AM400 spectrometer. The (HR-ESI) mass spectra were tested on a LCT Premier XE mass spectrometer. The UV-Vis absorption spectra were obtained on Agilent Technologies Cary 60 UV-Vis (1-cm quartz cell was used). The broadband visible light irradiations were performed by a handheld white LED lamp (YG-3896) with an output power of 1.5 W. The fluorescence spectra were recorded on a Varian Cray Eclipse fluorescence spectrophotometer.



Scheme 1. Synthetic routes of DASA-NDI

2.2 Synthesis of 4-bromo-N-butyl-1,8-naphthalimide **2**

The mixture of 4-bromo-1,8-naphthalic anhydride **1** (4.00 g, 14.44 mmol) and n-butylamine (10.60 g, 0.14 mol) in ethanol (40 mL) was refluxed under argon for 8 h. After being cooled, the mixture was poured into water, and the precipitate was collected by filtration and then recrystallized from acetic acid (4.40 g, 91.7%). ^1H NMR (CDCl_3 , 400 MHz, 298K), δ (ppm): 8.66 (d, $J = 8.0$ Hz, 1H), 8.57 (d, $J = 8.0$ Hz, 1H), 8.42 (d, $J = 8.0$ Hz), 8.04 (d, $J = 8.0$ Hz, 1H), 7.85 (t, $J = 8.0$ Hz, 1H), 4.18 (t, $J = 7.6$ Hz, 2H), 1.68-1.75 (m, 2H), 1.40-1.50 (m, 2H), 0.98 (t, $J = 7.6$ Hz, 3H).

2.3 Synthesis of N-butyl-1,8-naphthalimide borate **3**

The solution of 4-bromo-N-butyl-1,8-naphthalimide **2** (500 mg, 1.51 mmol) and bis(pinacolato)diboron (1.10 g, 4.33 mmol) in dry dioxane (40 mL) was mixed with potassium acetate (443 mg, 4.52 mmol), [1,1'-bis(diphenylphosphino)f

errocene]dichloropalladium (50 mg, 0.07 mmol), and the mixture was heated to 85 °C under argon atmosphere. After 12 h reaction, it was cooled down and poured into water (100 mL), then extracted with dichloromethane (50 mL × 3), and the organic layer was separated and concentrated in vacuum. The residue was purified by column chromatography on silica gel (petroleum ether: dichloromethane = 1:1) to afford white powder (500 mg, 87.6%). ¹H NMR (CDCl₃, 400 MHz, 298K), δ (ppm): 9.10 (d, *J* = 7.6 Hz, 1H), 8.60 (d, *J* = 7.6 Hz, 1H), 8.56 (d, *J* = 7.6 Hz, 1H), 8.29 (d, *J* = 7.6 Hz, 1H), 7.78 (t, *J* = 7.6 Hz, 1H), 4.19 (t, *J* = 7.6 Hz, 2H), 1.69-1.77 (m, 2H), 1.41-1.50 (m, 2H), 1.45 (s, 12H), 0.98 (t, *J* = 7.6 Hz, 3H).

2.4 Synthesis of 5- (*N*-butyl-1,8-naphthalimide)-indoline **4**

A stirred solution of *N*-butyl-1,8-naphthalimide borate **3** (100mg, 0.27 mmol) and 5-bromoindoline (45.22 mg, 0.23 mmol) in dioxane (15 mL) 5-bromoindoline charged with 2 M K₂CO₃ aqueous solution (5 mL), tetrakis(triphenylphosphine)palladium (Pd(PPh₃)₄) (21 mg, 0.02 mmol), and the mixture was heated to 100 °C under argon atmosphere. After 2 h stirring at this temperature, it was cooled and poured into water (15 mL), then extracted with dichloromethane (15 mL × 3), the organic layer was separated, and washed with saturated brine solution and dried over MgSO₄, then concentrated in vacuum. The residue was purified by column chromatography on silica gel (petroleum ether: ethyl acetic =10:1) to obtain pale yellow solid in 56% yield (57 mg). ¹H NMR (CDCl₃, 400 MHz, 298K), δ (ppm): 8.61(m, 2H), 8.41 (dd, *J* = 4.4, 0.8 Hz, 1H), 7.67 (m, 2H), 7.27

(d, $J = 8.0$ Hz, 1H), 7.17 (dd, $J = 8.0, 4.0$ Hz, 1H), 6.78 (d, $J = 8.0$ Hz, 1H), 4.20 (t, $J = 7.6$ Hz, 2H), 3.69 (t, $J = 4.4$ Hz, 2H), 3.15 (t, $J = 8.2$ Hz, 2H), 1.73 (m, 2H), 1.45 (m, 2H), 1.0 (t, $J = 8.0$ Hz). ^{13}C NMR (CDCl_3 , 100 MHz), δ (ppm): 163.5, 163.3, 151.1, 146.8, 132.1, 130.0, 129.9, 129.2, 128.8, 128.6, 128.0, 127.9, 126.5, 125.3, 121.8, 119.7, 112.4, 108.8, 108.0, 59.4, 46.5, 39.2, 29.2, 28.6, 26.8, 19.4, 12.8. HRMS (ESI) (m/z): $[\text{M}+\text{H}]^+$ calcd for $\text{C}_{24}\text{H}_{23}\text{N}_2\text{O}_2$, 371.1754; found, 371.1751.

2.5 *Synthesis* of
 5-((2Z,4E)-5-(5-(2-butyl-1,3-dioxo-2,3-dihydro-1H-benzo[de]isoquinolin-6-yl)indolin-1-yl)-2-hydroxypenta-2,4-dien-1-ylidene)-1,3-dimethylpyrimidine-2,4,6(1H,3H,5H)-trione **6**

A mixture of 5-(N-butyl-1,8-naphthalimide)-indoline **4** (40 mg, 0.11 mmol) and barbutaric acid furan adduct **5** (23.4 mg, 0.1 mmol) was stirred at room temperature in DCM (1 mL) until the reaction was completed (monitored by TLC). The crude mixture was added with DCM (1 mL) and sonicated for 1 min. The mixture was then added to vigorously stirring hexane (50 mL) dropwise. The product was filtered and washed with hexane to afford blue crystals in 72% yields (44 mg). The equilibrium state of **DASA-NDI** includes 22% isomer **6** and 78% isomer **7** (Fig. S6-S7). NMR characterization is cyclized **DASA-NDI 7**. ^1H NMR (CDCl_3 , 400 MHz, 298K), δ (ppm): 8.61 (m, 2H, naphthalene-H), 8.37 (dd, $J = 8.0, 4.0$ Hz, 1H, naphthalene-H), 7.73 (m, 1H, naphthalene-H), 7.69 (m, 1H, naphthalene-H), 7.64(m, 1H, indoline-H), 7.18(m, 1H, indoline-H), 6.61 (m, 1H, indoline-H), 6.48 (dd, $J_1 = J_2 = 8.0$ Hz, 1H,

cyclopentenone-H), 5.50 (m, 1H, cyclopentenone-H), 4.22 (t, $J = 8.0$ Hz, 2H, naphthalene-H), 4.05 (m, 1H, barbaturic acid-H), 3.83 (m, 1H, cyclopentenone-H), 3.66 (m, 2H, indoline-H), 3.44 (m, 1H, cyclopentenone-H), 3.38 (s, 3H, barbaturic acid-H), 3.19 (s, 3H, barbaturic acid-H), 3.16 (m, 2H, indoline-H), 1.73 (m, 2H, naphthalene-H), 1.47 (m, 2H, naphthalene-H), 0.98 (t, $J = 8.0$ Hz, 3H, naphthalene-H). ^{13}C NMR (CDCl_3 , 100 MHz), δ (ppm): 202.9, 167.2, 166.8, 164.4, 164.2, 162.5, 151.1, 150.9, 147.2, 134.8, 132.8, 131.1, 131.0, 130.6, 130.1, 129.6, 128.9, 127.5, 127.0, 126.5, 126.5, 123.0, 121.0, 106.0, 60.1, 48.1, 47.6, 46.8, 40.2, 30.2, 29.0, 28.7, 28.1, 20.4, 13.9. HRMS (ESI) (m/z): $[\text{M-H}]^+$ calcd for $\text{C}_{39}\text{H}_{31}\text{N}_4\text{O}_6$, 603.2249; found, 603.2239. (For details, see Support Information, Fig. S4-S8).

3 Results and discussion

3.1 Spectral properties

3.2.1 Photochromic properties of **DASA-NDI**

The photochromic characteristics of **DASA-NDI** have been measured in three different solvents at 293 K with alternating irradiation by broadband visible light and heat in 310 K, and its representative absorption spectra and fluorescence spectra are shown in Table 1. The absorption bands for indoline-DASA was approximately at 616 nm and 438 nm in different solvents, which was consistent with the absorption of native indoline-DASA ($\lambda_{\text{max}} = 615$ nm) in previous report [15]. Besides, compared with the absorption band of **4** ($\lambda_{\text{max}} = 360$ nm), the reason for bathochromic shift in absorption band of **DASA-NDI** ($\lambda_{\text{max}} = 438$ nm) might be homoconjugation that

enhanced hybridization of molecular orbitals between the electron-rich donors and acceptor groups (Fig. 2, Fig. S9).

The molar absorptivities (ϵ) for **DASA-NDI** in toluene, trichloromethane and acetonitrile were determined through a combination of NMR and absorption spectroscopies at equilibrium state, uniformly high at $\sim 10^6 \text{ M}^{-1} \text{ cm}^{-1}$, which agrees with the previous investigation and proves that the change of colour between dilute solutions of the two states could be visually monitored easily [15] (Fig. S10, Table S1). Moreover, as is shown in ^1H NMR spectroscopy, the percentage of open form of **DASA-NDI** in CDCl_3 was ca. 22 % at equilibrium state, which was essential in observing the photochromic properties. Additionally, the key signals at $\delta = 12.44, 8.26, 7.47, 7.41$ ppm were attributed to the protons on triene of open isomer **6** ($\text{H}_{\text{a-d}}$). Upon visible light irradiation, these signals were disappeared and the chemical shifts at $\delta = 6.48, 5.50, 4.05, 3.83, 3.44$ ppm were attributed to the protons on cyclopentenone or barbaturic acid ($\text{H}_{\text{a'-d'}}$). (Fig. S7)

Upon continued irradiation with visible light, the green solution of **DASA-NDI** in CHCl_3 was converted into pale yellow, and the absorption band of it decreased at 623 nm but increased at 442 nm with the blue shift of the absorption band, which is due to the reversible thermal 4π electrocyclic reaction. After being placed at 35°C for 20 min, the color of solution returned green and the absorption spectra nearly recovered to its initial state (Fig.2a and 2c). Moreover, ^1H NMR spectroscopy and absorption spectroscopy indicating that the opening and closing rates and activation energies (E_{A}) of **DASA-NDI** were comparable to experimental results obtained by Alaniz (Table 1)

[15].

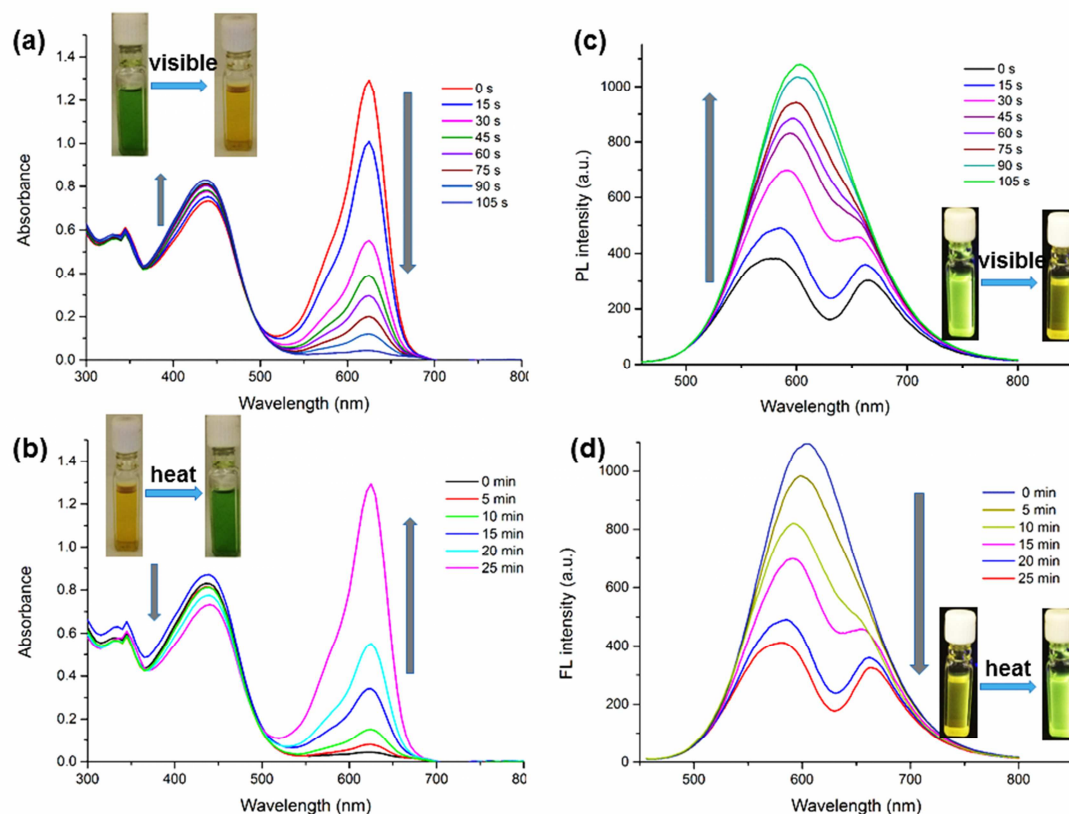


Figure 2. Absorption spectral changes (a, b) and fluorescence spectral changes (c, d) of DASA-NDI upon irradiation with broadband visible light (1.5 mW/ cm^2) in CHCl_3 ($5.5 \times 10^{-4} \text{ M}$) and upon heating at 35°C after irradiation. The irradiation time for each step was 15 s. The heat time for each step was 5 min.

Entry	Photochromism				Fluorescence				
	Solvent	λ_A nm (ϵ , $\text{L mol}^{-1} \text{cm}^{-1}$)	E_{open} (kJ/mol)	E_{closed} (kJ/mol)	Cyclization rate (s^{-1}) *100	λ_{ex} (nm)	λ_{em} (nm)	ϕ_{open}	ϕ_{closed}
1	Toluene	438 ($3.4 \cdot 10^5$) 616 ($3.0 \cdot 10^5$)	60	65	2.84	438	534	0.21	0.56

2	Trichloromethane	442 ($1.2 \cdot 10^6$)	58	63	2.91	442	654	0.2	0.4
		623 ($1.1 \cdot 10^6$)					594	3	6
							604		
3	Acetonitrile	441 ($8.5 \cdot 10^5$)	57	61	2.87	441	573	0.0	0.0
		619 ($4.6 \cdot 10^5$)						2	2
Alaniz [15]	CD_2Cl_2	615 ($1.1 \cdot 10^5$)	63	68	2.96	---	---	---	

Table 1. Spectral characteristics of initial and photoinduced forms of **DASA-NDI 6, 7** in different solvents (5.5×10^{-5} M) at 298K.

In order to examine the reversibility and stability of **DASA-NDI** in trichloromethane, an extensive cycling test was performed via Pump-probe absorption spectroscopy with a broadband white LED for excitation and a heated stage for equilibration (35 °C in trichloromethane, 22% open form at equilibrium state indicated by 1H NMR spectrum). During the first cycle, a detailed plot of absorption at λ_{max} (623 nm) was shown in Fig. 1b, and the following 10 cycles were measured by following photostationary state and thermal equilibration (Fig.1c). Through fatigue experiments, this rapid and complete switching of **DASA-NDI** (5% loss after 10 cycles) demonstrated the robust nature of this progress.

3.2.2 Fluorescent properties of **DASA-NDI** under visible light/heat and H^+/Cu^{2+}

The significant absorbance changes in the visible region, associated with the photoinduced transformation of a triene to cyclopentenone, can be exploited to activate an energy-transfer pathway and control the emission of the fluorescent partner.

As is shown in Fig. 2, upon irradiation with visible light ($\lambda = 442$ nm) in CHCl_3 solution, the **DASA-NDI** can be activated, and two fluorescence bands appear in the wavelength region of 520-620 nm for closed-ring isomer **7** and 620-720 nm for **6**, respectively. The initial state including **6** and **7** gave relatively weak fluorescence. Meanwhile, the peak absorption of **DASA-NDI** was around 620 nm and the significant overlap between it and the emission of the isomer **7** permits the transfer of energy from the fluorescent to the photochromic fragment, which results in the lower fluorescence intensity. However, upon brand visible light illumination for 105 s, the triene switches to the corresponding cyclopentenone to form **7** with the decrease of characteristic absorption of **6** ($\lambda = 620$ nm), the absorption at the wavelength of 442 nm enhanced, and the disappearance of corresponding emission band ($\lambda = 620-720$ nm), leading to the enhancement of fluorescence intensity. All these changes are due to the lack of any overlap between the emission of the fluorophore and the absorption of the photochrome that prevents the transfer of energy.

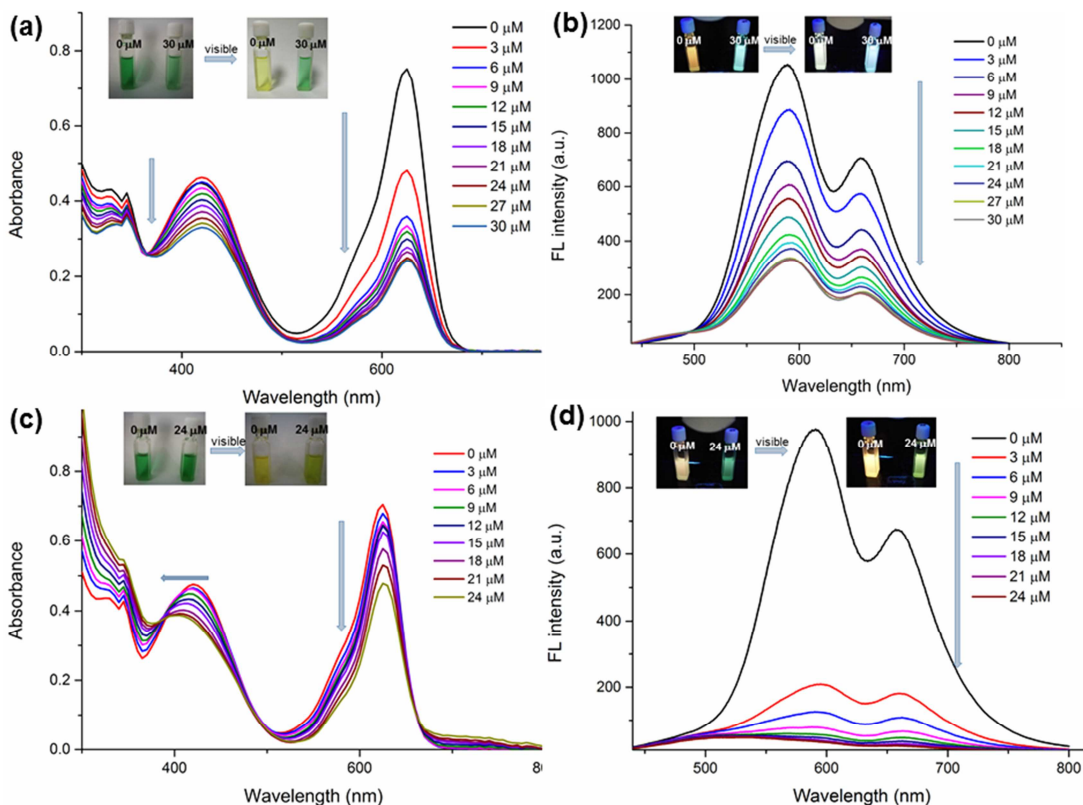


Figure 3. The absorption spectral and fluorescence spectral changes of **DASA-NDI** in CHCl_3 solution (20 μM) upon addition of various amounts of H^+ (a, b) and Cu^{2+} (c, d). Moreover, corresponding photographs before and after illumination with visible light also shown on the top of spectra. Cu^{2+} is derived from cupric acetate ($\text{Cu}_2(\text{OAc})_4$) and dissolved in the mixed solvent of $\text{CHCl}_3/\text{MeOH}$ (3:2) and H^+ is derived from CF_3COOH and dissolved in CHCl_3 .

Besides, the fluorescence quantum yields of the **DASA-NDI** (ϕ_{open} and ϕ_{closed}) in various solvents, using Rhodamine B (RhB) in 0.1 M EtOH as a reference, showing that both the emission intensity and quantum yields were sensitive to visible light, namely, the parameters increase under visible light irradiation (Table 1, Fig. S11) [29]. Moreover, after 105 s illumination, the photostationary state **7** has a lifetime of 25 min under heating in 35°C and eventually reverts back to the mixture of original isomer **6** and **7**. As a result, the initial absorption and emission spectra were almost fully restored in a few minutes under heat.

Furthermore, upon addition of various amounts of H^+ in $CHCl_3$ solution of **DASA-NDI**, the intensity of the absorption band at 430 nm and 623 nm decreased and the fluorescence intensity at 589 nm and 660 nm declined continuously. The two solutions of **DASA-NDI** before and after adding 30 μM H^+ showed green color, but upon irradiation of two green solutions with visible light, the solution without acid addition became yellow and its fluorescence intensity was significantly enhanced, yet the other with the addition acid did not change at all. The reason for this difference is that the acid protonates the tertiary amine on the indoline which results in the prohibition of the photo-induced isomerization of **DASA-NDI** (Fig. 3a-3b). Besides, upon adding different amounts of Cu^{2+} in $CHCl_3$ solution of **DASA-NDI**, the intensity of the absorption bands at 430 nm and 623 were decreased a bit and the absorption band at 430 nm shifted to blue obviously and the fluorescence intensity at 589 nm and 660 nm declined sharply, which is due to the weak coordination effect of copper ions and tertiary amines on the indoline. Significantly, as shown in Fig.3c and 3d, after irradiation of **DASA-NDI** and **DASA-NDI-Cu²⁺** with visible light, the former became yellow and the later became yellow-green due to the influence of ions, but the fluorescence intensity of **DASA-NDI-Cu²⁺** increased remarkably, which is probable due to the photoisomerization that destructs the weak coordination between copper ions and nitrogen atoms.

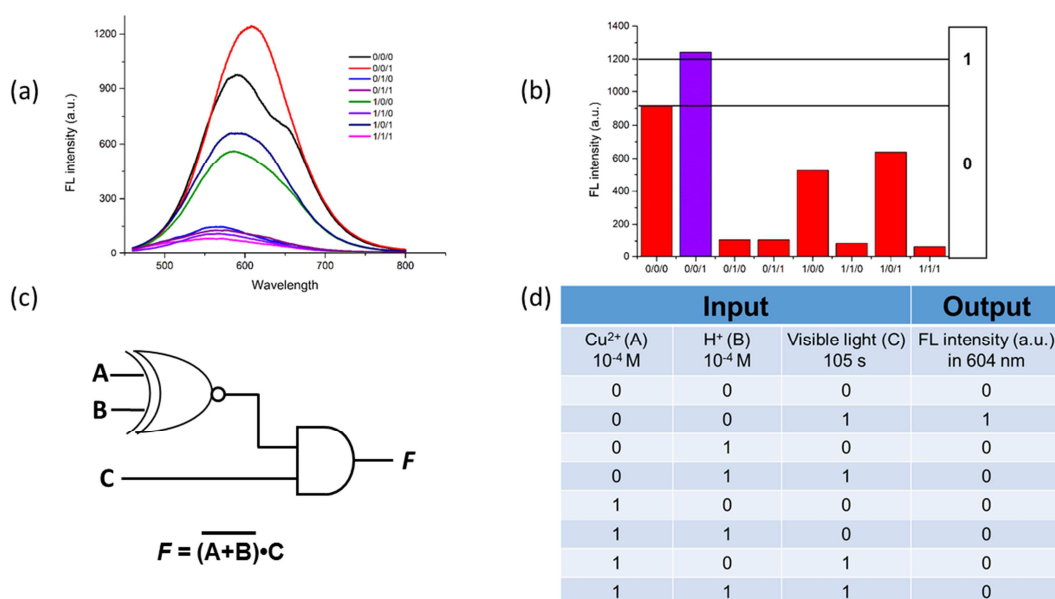


Figure 4. The DASA-NDI-based combinational (NOR and AND) logic gate; (a) The fluorescence spectra of DASA-NDI under different inputs and (b) their corresponding value of FL intensity at 604 nm. (c) Design strategy and logical expression. Only in the presence of visible light input (0/0/1), the FL intensity increased (output = 1), otherwise output was “0”. (d) A truth table of the combinational logic gate.

3.2.3 Fluorescent photochromic switch and logic gate

As a basic binary unit, the fluorescent chemosensor combined with a molecular switch offers a possibility for establishing electronic logic devices. Based on the new fluorescent photochromic switch (DASA-NDI), a combinational (NOR and AND) logic gate system can be designed (Fig. 4c). With respect to inputs, the presence and absence of broadband visible light irradiation as well as the addition of Cu²⁺ and the control of H⁺ was defined as “1” and “0”, respectively. The fluorescence of DASA-NDI, acting as outputs, can be controlled by using visible light, H⁺ or Cu²⁺ to switch between the open (low-fluorescent, $I \leq 1000$) and closed (high-fluorescent, $I \geq 1000$) state, where I is the value of fluorescence intensity at 604 nm. If the value of I

locates under 1000, the corresponding output is considered as the “1” state, otherwise, it is considered as the “0” state (Fig. 4a and Fig. 4b).

Therefore, according to the truth table shown in Fig. 4d, a combinatorial logic gate integrated within a single molecule was approached. Only the presence of visible light input (0/0/1) could enhance the fluorescence intensity of **DASA-NDI** (output = 1) indicated complete photoisomerization of **DASA-NDI**; while those in the absence and presence of three inputs (0/0/0, 1/1/1) or in the presence of either input expect visible light or both inputs (1/0/0, 0/1/0, 0/1/1, 1/0/1, 1/1/0) remain low-fluorescent or nearly non-fluorescent, which can be confirmed by testing the fluorescence intensity responses (Fig. 4a-4b).

Conclusion

In conclusion, a novel fluorescent photochromic **DASA-NDI** whose fluorescence could be flexibly controlled by visible-light/heat and ions/protons were successfully designed and conveniently synthesized by Suzuki-Miyaura coupling of combining a fluorescent unit, 1,8-naphthalimide and a second generation DASA photoswitch. The photochromic and fluorescent properties of **DASA-NDI** have been investigated under certain visible light in different solvents, which results in the application of a reversible fluorescent photoswitch and a combinatorial (NOR and AND) logic gate. We envision that this novel visible light strategy will afford an efficient and green method for construction of photochromic fluorescent switching and advance the study of various photoswitches.

Acknowledgement

We thank the support of NSFC/China (21672060), the Fundamental Research Funds for the Central Universities (WJ1616011, WJ1213007, 222201717003), the Programme of Introducing Talents of Discipline to Universities (B16017).

Appendix A. Supplementary data

Supplementary data related to this article can be found at

Reference

- [1] Estabrook RW, Maitra PK. A fluorimetric method for the quantitative microanalysis of adenine and pyridine nucleotides. *Anal Biochem* 1962; 3: 369–382.
- [2] Stender AS, Marchuk K, Liu, C, Sander S, Meyer MW, Smith E A, et al. Single cell optical imaging and spectroscopy. *Chem Rev* 2013; 113: 2469–2527.
- [3] Fukaminato T, Doi T, Tamaoki N, Okuno K, Ishibashi Y, Miyasaka H, Irie M. Single-molecule fluorescence photoswitching of a diarylethene-perylenebisimide dyad: non-destructive fluorescence readout. *J Am Chem Soc* 2011; 133: 4984–4990.
- [4] Irie M, Fukaminato T, Sasaki T, Tamai N, Kawai T. Organic chemistry: a digital fluorescent molecular photoswitch. *Nature* 2002; 420: 759–760.
- [5] Prakash K, Sahoo PR, Kumar S. A fast, highly selective and sensitive anion probe stemmed from anthracene-oxazine conjugation with CN⁻ induced FRET. *Dyes Pigments* 2017; 143: 393–400
- [6] Cong BF, Le LG, Huang L, et al. Significant enhancement of C₂H₂/C₂H₄ Separation by a photochromic diarylethene unit: A temperature- and light-responsive separation switch. *Angew Chem Int Ed* 2017; 129: 8008–8014.
- [7] Meng XS, Gui B, Yuan DQ, Zeller M, Wang C. Mechanized azobenzene-functionalized zirconium metal-organic framework for on-command cargo release. *Sci Adv* 2016; 2: e1600480.
- [8] Berkovic G, Krongauz V, Weiss V. Spiropyrans and spirooxazines for memories

- and switches. *Chem Rev* 2000; 100:1741–1754.
- [9] Yokoyama Y. Fulgides for Memories and Switches. *Chem Rev* 2000; 100:1717–1740.
- [10] Sallenave X, Delbaere S, Vermeersch G, Saleh A, Pozzo JL. Photoswitch based on remarkably simple naphthopyrans. *Tetrahedron Lett* 2005; 46: 3257–3259.
- [11] Hu L, Duan Y, Xu Z, Yuan J, Dong Y, Han T. Stimuli-responsive fluorophores with aggregation-induced emission: implication for dual-channel optical data storage. *J Mater Chem C* 2016; 4: 5334–5341.
- [12] Qu DH, Ji FY, Wang QC, Tian H. A double Inhibit logic gate employing configuration and fluorescence changes. *Adv Mater* 2006; 18: 2035–2038.
- [13] Mariam, EK, Alexandre M., Dominique B, Jacques-Philippe C, Virgile A. Rational design of ultrastable and reversibly photoswitchable fluorescent proteins for super-resolution imaging of the bacterial periplasm. *Sci Rep* 2016; 6: 18459.
- [14] Majumdar D, Han ML, Kim J, Kim KS, Mhin BJ. Photoswitch and nonlinear optical switch: theoretical studies on 1, 2-bis-(3-thienyl)-ethene derivatives. *J Chem Phys* 1999; 111: 5866–5872.
- [15] Hemmer JR, Poelma SO, Treat N, Page ZA, Dolinski N, Diaz YJ, et al. Tunable visible and near infrared photoswitches. *J Am Chem Soc* 2016; 138: 13960–13966.
- [16] Helmy S, Leibfarth FA, Oh S, Poelma JE, Hawker CJ, Read dAJ. Photoswitching using visible light: a new class of organic photochromic molecules. *J Am Chem Soc* 2014; 136: 8169–8172.
- [17] Helmy S, Oh SS, Leibfarth FA, Hawker CJ, Read dAJ. Design and synthesis of donor—acceptor stenhouse adducts: a visible light photoswitch derived from furfural. *J Org Chem* 2014; 79: 11316–11329.
- [18] Lerch MM, Wezenberg SJ, Szymanski W, Feringa BL. Unraveling the photoswitching mechanism in donor-acceptor stenhouse adducts. *J Am Chem Soc* 2016; 138: 6344–6347.
- [19] Poelma SO, Oh SS, Helmy S, Knight AS, Burnett GL, Soh HT, et al. Controlled drug release to cancer cells from modular one-photon visible light-responsive micellar system. *Chem Commun* 2016; 52:10525–10528.
- [20] Mallo N, Brown PT, Iranmanesh H, Macdonald TS, Teusner MJ, Harper JB, et al. Photochromic switching behaviour of donor-acceptor stenhouse adducts in

- organic solvents. *Chem Commun* 2016; 52: 13576–13579.
- [21] Weinhold F. Chemistry: A new twist on molecular shape. *Nature*, 2001; 411: 539–541
- [22] Jin Chao, Wang YG, Qian HF. A Cu(II) complex with 2,9-Dithienyl-1,10-phenanthroline-5,6-dione Ligand with large steric hindrance. *Chinese J Inorg Chem*, 2015; 31:413–419.
- [23] Diaz YJ, Page ZA, Knight AS, Treat NJ, Hemmer JR, Hawker CJ, et al. A versatile and highly selective colorimetric sensor for detection of amines. *Chem Eur J* 2017; 23: 3562–3566
- [24] Lerch MM, Hansen MJ, Velema WA, et al. Orthogonal photoswitching in a multifunctional molecular system. *Nat Commun* 2016; 7:12054.
- [25] Jia S, Du JD, Hawley AM, Fong WK, Graham B, Boyd BJ. Investigation of donor acceptor stenhouse adducts as new visible wavelength-responsive switching elements for lipid-based liquid crystalline systems. *Langmuir* 2017; 33:2215–2221.
- [26] Balamurugan A, Lee H. A visible light responsive on–off polymeric photoswitch for the colorimetric detection of nerve agent mimics in solution and in the vapor phase. *Macromolecules* 2016; 49: 2568–2574.
- [27] Singh S, Friedel K, Himmerlich M, Lei Y, Schlingloff G, Schober A. Spatiotemporal photopatterning on polycarbonate surface through visible light responsive polymer bound dasa compounds. *Acs Macro Lett* 2015; 4: 1273–1277
- [28] Sinawang G, Wu B, Wang J, Li S, He Y. Polystyrene based visible light responsive polymer with donor–acceptor stenhouse adduct pendants. *Macromol Chem Phys* 2016; 217: 2409–2414.
- [29] Yang X, Pan ZT, Ma Y. Rhodamine B as standard substance to measure the fluorescence-quantum yield of dichlorofluorescein. *J Anal Sci* 2003; 19: 588-589.

Highlights

A novel photochromic donor-acceptor Stenhouse adduct was successfully constructed for fluorescent photoswitch.

.

The photochromic fluorescent switch could be flexibly tuned not only by visible-light/heat but also by ions/protons.

A combinatorial logic gate consisting of NOR and AND logics was further constructed based on the favorable optical and chemical properties of the adduct.